

# Point Mutations In *Candida Glabrata* 3-Hydroxy-3-Methyl Glutaryl Coenzyme A Reductase (HMGR Cg) An Antifungal Target, Decrease Enzymatic Activity And Substrate/Inhibitor Affinity

**Dulce Andrade-Pavón**

Instituto Politécnico Nacional

**Vanessa Fernández-Muñoz**

Instituto Politécnico Nacional

**Wendy González-Ibarra**

Instituto Politécnico Nacional

**César Hernández-Rodríguez**

Instituto Politécnico Nacional

**J. Antonio Ibarra**

Instituto Politécnico Nacional

**Lourdes Villa-Tanaca** (✉ [mvillat@ipn.mx](mailto:mvillat@ipn.mx))

Instituto Politécnico Nacional

---

## Research Article

**Keywords:** HMGR mutants, *Candida glabrata*, Site-directed mutagenesis, Docking, EC 1.1.1.34

**Posted Date:** June 29th, 2021

**DOI:** <https://doi.org/10.21203/rs.3.rs-618523/v1>

**License:** © ⓘ This work is licensed under a Creative Commons Attribution 4.0 International License.

[Read Full License](#)

---

# Abstract

An alternative target for antifungal drugs is 3-hydroxy-3-methyl glutaryl coenzyme A reductase (HMGR), a key enzyme in the ergosterol biosynthesis pathway. The aim of this study was to obtain, purify, characterize, and overexpress five point mutations in highly conserved regions of the catalytic domain of *Candida glabrata* HMGR (HMGR<sub>Cg</sub>) to explore the function of key amino acid residues. Glutamic acid (Glu) was substituted by glutamine in the E680Q mutant (at the dimerization site), Glu by glutamine in E711Q (at the substrate binding site), aspartic acid by alanine in D805A and methionine by arginine in M807R (the latter two at the cofactor binding site). A double mutation, E680Q-M807R, was also made. The *in vitro* enzymatic activity decreased significantly in all recombinant (versus wild-type) HMGR<sub>Cg</sub>, and the *in silico* binding energy for simvastatin, alpha-asarone and the substrate HMG-CoA was also lower for the mutants. The lowest enzymatic activity and binding energy was displayed by E711Q, suggesting that Glu<sup>711</sup> (in the substrate binding site) is an important residue for enzymatic activity. The double mutant HMGR<sub>Cg</sub> E680Q-M807R exhibited the second lowest enzymatic activity. The current findings provide insights into the role of residues in the catalytic site of HMGR<sub>Cg</sub>.

## Introduction

The ergosterol biosynthesis pathway has been proposed as a target for identifying and designing new antifungals. In a rate-limiting step of the biosynthetic pathway of ergosterol in fungi and cholesterol in humans, the enzyme 3-hydroxy-3-methylglutaryl-coenzyme A reductase (HMGR) catalyzes the conversion of 3-hydroxy-3-methylglutaryl-coenzyme A (HMG-CoA) to mevalonate.<sup>1</sup> This pathway also generates other bioactive molecules, including a coenzyme (Q10) that participates in the transport of electrons in mitochondria.<sup>2</sup>



Phylogenetic analyses have revealed two types of HMGR: class I of eukaryotic organisms and some archaea and class II of prokaryotes and some archaea. Whereas the first class has three domains (catalytic, linker and membrane-anchor), most members of the second one contain only the catalytic domain.<sup>1</sup>

The HMGR enzyme is the target of lipid-lowering drugs, such as statins.<sup>3</sup> These compounds have been described as competitive inhibitors because they dispute the active site with the substrate HMG-CoA.<sup>1</sup> Since statins can induce myopathy and hepatotoxicity,<sup>4</sup> new bioactive principles obtained from natural sources (e.g., alpha-asarone) have been synthesized. In a murine model, alpha-asarone decreased cholesterol and triglyceride levels. Moreover, its inhibitory effect was tested on the recombinant human HMGR enzyme and an enriched enzyme extract from *Schizosaccharomyces pombe*.<sup>5,6</sup>

The catalytic domain of HMGR of eukaryotic organisms is highly conserved and harbors the dimerization site, the substrate (HMG-CoA) binding site, and the cofactor (NADPH) binding site.<sup>1</sup> Hence, our group has

proposed fungal HMGR enzymes as a model for evaluating compounds with antifungal and hypocholesterolemic activity.<sup>7</sup> One of the fungi used for this purpose has been *Candida glabrata* because of its high incidence as an opportunistic pathogenic yeast in hospitalized patients with compromised immunity and its resistance to multiple conventional drugs, including azoles and echinocandins. This multi-drug resistance has led to treatment failures.<sup>8,9</sup>

In previous studies, the catalytic domain of the HMGR enzyme from *C. glabrata* (HMGRcG) was cloned, expressed and characterized, demonstrating its enzymatic activity as well as its inhibition by simvastatin and compounds derived from alpha asarone. Consequently, it has been proposed as an antifungal target.<sup>10,11</sup>

The recombinant HMGRcG enzyme is available and its catalytic activity is still under study. Therefore, the aim of the current contribution was to generate, characterize, and overexpress five point mutants of HMGRcG in order to explore the role of certain amino acid residues in the functioning of the catalytic domain of HMGRcG. Three highly conserved regions within the catalytic domain were mutated: the dimerization site, the substrate binding site, and the cofactor binding site.<sup>12</sup> Although point mutations have been investigated in the HMGR of other organisms, such as *Pseudomonas mevalonii* and Syrian hamsters, they have not been performed in the HMGR of fungi, much less in an opportunistic pathogenic yeast.<sup>12-16</sup>

## Results

### *Conservation of the sites of interest in the catalytic domain of HMGRs from different organisms*

A multiple alignment of the amino acid sequence was carried out on the Clustal Omega program for the soluble fraction of HMGR from plants, bacteria, insects, mammals (including *H. sapiens*), and opportunistic pathogenic yeasts (e.g., *C. glabrata*) (Supplementary Fig. S1). The motif sequences in the sites of interest in the HMGR enzymes are highlighted (Fig. 1): the dimerization site (ENVIG), the substrate binding site (EGCLVAS), and the cofactor binding site (DAMGMN). The amino acid sequences encoding the soluble fraction of the HMGR enzymes of the different organisms are highly conserved, which emphasizes the importance of examining some of the amino acid residues in these sites in order to evaluate their role in the catalysis of the enzyme, as has been done in studies on *P. mevalonii*.

A phylogenetic tree was constructed by examining the amino acid sequences found in the catalytic domain of the twenty-four organisms included in the alignment test (Fig. 2). The phylogenetic analysis of HMGRcG demonstrated that it belongs to the clade of the yeast species of the Saccharomycotina subphylum and the *Saccharomyces* genus, not to the clade containing *C. albicans*.

### *Molecular modeling of wild-type and mutant HMGRcG proteins*

The homology modeling of the five mutants herein generated was carried out in the Modeller program, using the crystal structure of HMGR of *H. sapiens* (PDB: 1DQA) as the template. Of the fifteen models of

each mutant provided, the one with the lowest DOPE score (the most thermodynamically stable) was selected. The selected models are portrayed in (Fig. 3), highlighting in red the amino acids that were changed in the transition from the wild-type (Fig. 3a) to the mutant proteins (Fig. 3b,c,d,e and f): for E680Q, Glu66 to Gln66; for E711Q, Glu97 to Gln97; for D805A, Asp191 to Ala191, and for M807R, Met193 to Arg193.

The models were validated with the PROCHECK program, which quantifies the loss of residues in the allowed regions of a Ramachandran plot (Supplementary Fig. S2). In all the models, over 90% of the residues are found within the most favorable regions, with no residues in the disallowed regions (Supplementary Table 1). All the models constructed had Ramachandran statistics similar to those reported in the wild-type HMGRc model. These results confirmed the high quality and reliability of the models generated.

#### *Docking study of ligand binding to wild-type and mutant HMGR proteins*

An *in-silico* analysis was carried out for the interaction of mutant and wild-type HMGRc proteins with two of their inhibitors (simvastatin and alpha-asarone) and their substrate (HMG-CoA) (Fig. 4). Each of the mutants had lower binding energies than that of the wild-type HMGRc (Fig. 4, Table 2). The mutant protein E711Q displayed the lowest value (Fig. 4). Glu97, Asp307, Lys321 and His403 are the residues most frequently involved in binding, being located in the catalytic domain of HMGRc. However, the aforementioned amino acids are not involved in the binding of the ligands with some of the mutant peptides (Table 2).

Regarding the binding of simvastatin, alpha asarone and HMG-CoA to the active site of the HMGRc enzyme, the docking simulations gave insights into the binding energies as well as the residues, polar interactions, and hydrophobic interactions involved (Table 1).

Table 1

Results of docking simvastatin, alpha asarone and HMG-CoA at the active site of HMGR of *Candida glabrata* (HMGRcG).

Protein	Compound	Binding energy $\Delta G$ (kcal/mol)	Residues interacting with the ligand	Polar interactions	Hydrophobic interactions
<b>Wild-type HMGRcG</b>	Simvastatin	-10.71	Glu97, Met193, Asp307	Glu97, Met193, Asp307	Met193
	Alpha- asarone	-6.4	Thr96, Glu9, Ala192, Met193, Met197, Gly305, Gln306, Gln310, Thr346	Glu97, Gln306, Thr346	Ala192, Met197
	HMG-CoA	-6.48	Asp128, Lys231, Lys275, Asn407	Lys231, Lys275, Asn407	Asp128
<b>HMGRcG E680Q</b>	Simvastatin	-10.18	Ala192, Met193, Asn196, Asp307, Gly344, Gy345, His403	Asn196, Asp307	Ala192, His403
	Alpha- asarone	-5.81	Asp230, Lys231, Lys275, Asn290, Ser315	Asp230, Asn290, Ser315	Lys275
	HMG-CoA	-6.31	Arg128, Ser224, Asp230, Lys231, Lys232, Lys275	Ser224, Asp230	Lys232, Lys275
<b>HMGRcG E711Q</b>	Simvastatin	-7.1	Gly98, Arg128, Lys231, His292, Asn295, Leu390, Leu394, Leu399	Gly98, Arg128, His292, Asn295, Leu399, His403	Lys231, Leu390
	Alpha- asarone	-5.7	Lys231, Lys232, Pro233, Gly288, Ala294, Ser315, Asn316	Gly288, Ser315	Lys232, Pro233, Ala294, Asn316
	HMG-CoA	-6.05	Arg128, Ser224, Asn226, Lys232, Lys275	Ser224, Lys232, Lys275	Arg128, Lys232
<b>HMGRcG D805A</b>	Simvastatin	-9.54	Leu74, Leu302, Asp307	Asp307	Leu74, Leu302
	Alpha- asarone	-6.33	Arg128, Ser199, Leu399, His403, Met404, Val498	Arg128, Ser199	Leu399, His403, Val498
	HMG-CoA	-6.26	Asn196, Ser199, Lys200, Glu203, His403, Arg408	Glu203, Ser199, His403	Glu203, His403
<b>HMGRcG M807R</b>	Simvastatin	-9.78	Glu97, Arg128, Val223, Asp230, Asn295, Leu399, Val400, His403	Glu97, Asp230	Val223, Val400

Protein	Compound	Binding energy $\Delta G$ (kcal/mol)	Residues interacting with the ligand	Polar interactions	Hydrophobic interactions
	Alpha- asarone	-6.86	Glu97, Lys231, Lys232, Ala293, Ala294, Asn295	Lys232	Glu97, Lys232, Ala293, Ala294, Asn295
	HMG-CoA	-6.35	Arg106, Leu399, His403	Arg106, Leu399, His403	—
<b>HMGR</b> <b>Cg</b> <b>E680Q-</b> <b>M807R</b>	Simvastatin	-7.36	Ala63, Cys64, Glu97, Asp307, Arg408	Glu97, Asp307	Ala63, Cys64, Arg408
	Alpha- asarone	-5.8	Lys231, Pro233, Val286, Ala294	—	Lys231, Pro233, Val286, Ala294
	HMG-CoA	-6.13	Cys65, Val68, Ile69, Tyr71, Thr95, Thr96	Cys65, Val68, Ile69, Tyr71, Thr95, Thr96	—

#### *Generation and verification of point mutants of HMGR genes*

PCR reactions were carried out with specific oligonucleotides designed to obtain the following mutants: HMGR<sub>Cg</sub>E680Q, HMGR<sub>Cg</sub>E711Q, HMGR<sub>Cg</sub>D805A, HMGR<sub>Cg</sub>M807R and HMGR<sub>Cg</sub>E680Q-M807R. The plasmid Rec-MBP-HMGR<sub>Cg</sub> was used as the template DNA (where MBP refers to the maltose-binding protein). The amplified oligonucleotides had a size of 7.9 kbp (Supplementary Fig. S3a), which corresponds to the size of the plasmid pMAL-C2X (6.6 kbp) plus the gene encoding the soluble fraction of the HMGR of *C. glabrata* (1.3 kbp); full-length gel original is included in Supplementary Information (Fig. S3c). Additionally, the plasmids afforded by the transformation of each of the amplified products were subjected to double digestion (Supplementary Fig. S3b), finding the expected molecules of 6.6 and 1.3 kbp; full-length blot is included in Supplementary Information (Fig. S3d).

Likewise, the mutations generated by sequencing were corroborated. The sequences obtained were aligned with the coding sequence of wild-type HMGR<sub>Cg</sub> to confirm that the corresponding mutations had indeed been introduced. For HMGR<sub>Cg</sub>E680Q and HMGR<sub>Cg</sub>E711Q, the triplet changed from GAA to CAA, though in different positions in each case. The GAT triplet changed to GCT in HMGR<sub>Cg</sub>D805A, and CAT to CCT in HMGR<sub>Cg</sub>M807R. For the double mutant HMGR<sub>Cg</sub>E680Q-M807R, TTC changed to TTG and CAT to CCT (Fig. 5). The sequencing revealed that the point mutations were introduced successfully.

#### *Expression, detection, and purification of HMGR<sub>Cg</sub> mutant proteins*

The protein expression of the HMGRcG E680Q, HMGRcG E711Q, HMGRcG D805A, HMGRcG M807R and HMGRcG E680Q-M807R mutants was induced with IPTG. Samples taken before and after induction were visualized on SDS-PAGE. The gel in (Fig. 6b) shows the overexpression of the proteins of interest. The approximate molecular mass of 90 kDa corresponds to the fusion of HMGRcG + MBP (Fig. 6a), because the pMAL vector favored the expression of the recombinant proteins, which fused to the soluble MBP. The latter facilitates the isolation of the enzyme after its overexpression.

Hence, the mutants were overexpressed and the presence of MBP fused to the mutants was verified. The mutants found were the same as those previously identified by using anti-MBP antibodies (Fig. 6c). Subsequently, the mutants were purified easily (in a few steps) by means of amylose affinity chromatography. In all cases, a single band appeared at the approximate molecular mass of 90 kDa, exhibiting the same behavior as wild-type HMGRcG.

#### *Reduced enzymatic activity for the mutants compared to wild-type Candida glabrata HMGR*

The enzymatic activity of the HMGRcG E680Q, HMGRcG E711Q, HMGRcG D805A, HMGRcG M807R and HMGRcG E680Q-M807R proteins was measured spectrophotometrically by reading the decrease in absorbance of NADPH at 340 nm during 10 min. For each mutant, this parameter was determined in triplicate and expressed as the percentage of activity of the wild-type protein (considered as 100%) (Table 2).

Compared to wild-type HMGRcG, all five mutants displayed a lower enzymatic activity. The smallest percentage of residual activity (23%) was observed for E711Q. The least affected enzyme was E680Q, mutated at the dimerization site, with 88.2% residual activity. The double mutant E680Q-M807R exhibited the second lowest activity (44%), compared to the 82% and 79% residual activity of the corresponding single mutants E680Q and M807R. The enzymatic activity of all mutants was significantly less than that of the wild-type protein, according to a paired Student's *t*-type analysis.

**Table 2.** The enzymatic activity and binding energies of the point mutations made in the motifs of the dimerization site, substrate binding site, and cofactor binding site of the *Candida glabrata* HMGR enzyme (HMGRcG).

Rec-HMGRcG Proteins	Point mutations, affected motif	Simvastatin	Alpha-asarone	HMG-CoA	Specific enzymatic activity	Percentage of HMGR activity
		Binding free energy (Kcal/mol)			(mU/mg of protein)	(% ± SD)
<b>HMGRcG-wild-type</b>		-10.71	-6.4	-6.48	13.6	100
<b>HMGRcG-E680Q</b> <b>Glu x Gln</b>	Dimer-ization ENVIG QNVIG	-10.18	-5.81	-6.31	11.2	82.2 ± 7.8***
<b>HMGRcG-E711Q</b> <b>Glu x Gln</b>	Substrate binding EGCLVAS QGCLVAS	-7.14	-5.7	-6.05	3.1	23.4 ± 7.8***
<b>HMGRcG-D805A</b> <b>Asp x Ala</b>	Cofactor binding DAMGMN AAMGMN	-9.54	-6.33	-6.26	7.0	51.7 ± 1.6***
<b>HMGRcG-M807R</b> <b>Met x Arg</b>	Cofactor binding DAMGMN DARGMN	-9.78	-6.86	-6.35	10.7	79 ± 2.1 **
<b>HMGRcG-E680Q-M807R</b> <b>Glu x Gln,</b> <b>Met x Arg</b>	Dimer-ization ENVIG QNVIG Cofactor binding DAMGMN DARGMN	-7.36	-5.8	-6.13	5.9	44 ± 9.8 *

Point mutations were made in the catalytic domain of HMGRcG to express various recombinant proteins (Rec-HMGRcG) (as described in Material and Methods). The aa of the wild-type sequence is shown in green and the mutated aa in red. The site of the motif sequence is indicated. The binding energies of HMGRcG (wild-type and mutated) with inhibitors (simvastatin and alpha-asarone) and the substrate HMG-CoA were estimated by docking. The enzymatic activity of the recombinant enzymes is calculated

as a percentage of the activity of the wild-type enzyme (considered as 100%). Data are reported as the average of three independent replicates  $\pm$  standard deviation (SD). \*\*\* P <0.0005 \*\* P <0.0052, \* P <0.0153. Significant differences compared to the wild-type protein based on a paired Student's *t*-type analysis.

## Discussion

HMGR is a highly conserved enzyme anchored to the endoplasmic reticulum membrane in eukaryotes and to the plasma membrane of prokaryotes. It is responsible for the synthesis of cholesterol in mammals, ergosterol in fungi, and isoprenoids in bacteria.<sup>1</sup> Intense research efforts have focused on human HMGR (HMGRh) as the target of inhibitors such as statins and fibrates, which diminish the synthesis of cholesterol and reduce the risk of cardiac arrest in patients with hyperlipidemia. Consequently, HMGRh has been examined at many levels: transcription, translational regulation, synthesis, inhibition, crystallization, and tertiary structure. However, reports on point mutations in non-human HMGR are limited, to the best of our knowledge, to *P. mevalonii* and Syrian hamsters. The current investigation is the first approach to making point mutations in the HMGR enzyme of a yeast of medical interest.

The alignment presently carried out with the amino acid sequences of HMGRs from various species demonstrated that the motif sequences of the dimerization site (ENVIG), the substrate binding site (EGCLVAS), and the cofactor binding site (DAMGMN) are highly conserved, regardless of whether they are from fungal, mammalian, plant or bacterial proteins. Hence, these amino acid residues appear to have an essential function in the catalysis reaction of the enzyme and/or in its conformation and tertiary structure, which makes them candidates for the evaluation of point mutants in key sequences. As a first approach to the study of the role played by some conserved aa in the three aforementioned motif sequences, the following five mutations were designed: HMGRcG-E680Q (dimerization site), HMGRcG-E711Q (substrate binding site), HMGRcG-D805A and HMGRcG-M807R (cofactor binding site), and a double mutant HMGRcG-E680, Q-M807R (dimerization and cofactor binding sites).<sup>12</sup>

On the other hand, the phylogenetic analysis of the HMGR proteins from different yeasts revealed a classification in accordance with their taxonomy. The majority are of the Phylum Ascomycota, which includes the *Candida* and *Saccharomyces* genus. HMGRcG was grouped with the yeast proteins of the WGD clade, encompassing *K. lactis* and *S. cerevisiae*,<sup>17,18</sup> and not with those of the CTG clade containing *C. albicans* and other *Candida* species. Therefore, *C. glabrata* is a species phylogenetically closer to *S. cerevisiae* than to *C. albicans*. The HMGRs of *Y. lipolytica*, *S. pombe* and *U. maydis* (the latter being a fungus of the phylum Basidiomycota) belong to branches completely independent of Ascomycota. The HMGRs of other eukaryotes such as plants, insects and mammals were grouped into an independent clade and the HMGR of the bacterium *P. mevalonii* functions as an external group, further validating the previous results.<sup>1</sup>

HMGRh, purified and crystallized in 2000, was used as a template for the molecular modeling of proteins.<sup>19</sup> Although the three-dimensional structure of the catalytic domain of HMGRh (426–888 aa) is a tetramer, it has been suggested that the protein dimer might be able to bind to the HMG-CoA substrate.<sup>19</sup> The dimer is known to be the conformation of the most stable bacterial HMGR. On the other hand, the oligomerization analysis of HMGRh revealed the presence of the ENVIG dimerization sequence, which is also found in the HMGR of *P. mevalonii*.<sup>19</sup>

The molecular modeling of the five HMGRcG with point mutations generated proteins made up of two identical subunits (dimers). In its wild type form, HMGRcG can catalyze HMG-CoA to mevalonate through the oxidation of NADPH.<sup>10,11</sup> The structures of the mutated proteins were validated by stereo-chemical restriction determinations on Ramachandran plots, thus providing an *a priori* approximation to the 3D structure of the corresponding peptides, a necessary step for their *in-silico* analysis.<sup>11</sup>

Statins and alpha-asarone are competitive inhibitors of HMGRs, blocking access to the HMG-CoA substrate.<sup>1,3,10,11</sup> Simvastatin (like other statins) and alpha-asarone have an HMG-like moiety capable of replacing the thioester oxygen atom found in the HMG-CoA substrate.<sup>3</sup> The HMGRcG mutant in the substrate binding motif, E711Q, displayed the lowest binding energies in relation to the ligands presently examined: simvastatin, alpha-asarone and the substrate HMG-CoA. It showed significantly lower enzymatic activity than the other mutants. The reduced enzymatic activity and binding energy of this mutant was not unexpected, considering that the three ligands currently tested interact with the EGCLVAS motif (of the substrate binding site).<sup>3,10,11</sup>

According to kinetic studies on HMGRh, statins compete for the substrate HMG-CoA without affecting binding to the cofactor NADPH.<sup>20</sup> Hence, the substitution of an amino acid residue in the conserved sequences could possibly alter the affinity of the enzyme for its substrate HMG-CoA as well as for simvastatin and alpha-asarone, to demonstrate this, a molecular docking study was carried out.

It is worth mentioning that it is the first report, to our knowledge, of molecular coupling between mutant proteins of HMGRcG and reference inhibitors. Information is provided on the substantial effect on the ligand-receptor interaction that is found after mutating specific amino acids.

The amino acids Glu97, Asp307, Lys321 and His403 are part of the of the catalytic domain of the HMGR of *C. glabrata* and their plausible role in the ligand-HMGR interaction has been proposed.<sup>1,11</sup> According to the docking studies the mutant enzymes underwent a change in conformation that altered the set of residues involved in ligand binding.

The amino acids affected by the mutations likely influenced the recognition of the substrate/inhibitor or altered the native structure of the protein.<sup>21</sup> Evidence of such a possibility is afforded by the highly conserved nature of HMGR and the significant effect on enzymatic activity produced by the mutation at all three sites (the dimerization, substrate binding, and cofactor binding sites).<sup>12</sup> Since the HMGRcG-E711Q mutant (at the substrate binding site) showed the greatest decrease in enzymatic activity,

glutamic acid in the EGCLVAS region seems to have an important function in the catalysis of HMGRcG. Future research is needed to confirm that the decrease in the enzymatic activity of rec-HMGRcG-E711Q is indeed due to the key role of amino acid E711 and not to a conformational change in the protein capable of impeding the recognition of the substrate.

HMGRcG-M807R was mutated at the cofactor binding site, specifically at the methionine position 807 of the DAMGMN sequence.<sup>12</sup> The change was from methionine, an amino acid with a neutral and nonpolar charge, to arginine, one with a positive charge. Although both amino acids participate in protein methylation,<sup>22</sup> the positive charge of arginine may be detrimental to the binding of the cofactor to the enzyme. Additionally, arginine contains a guanidinium group, which when ionized has a lower charge density than other amino acids. While methionine is a weak nucleophile and cannot be protonated,<sup>22</sup> the positive charge of arginine might be able to alter the  $\alpha$ -helix or  $\beta$ -folded structure of the protein and consequently the enzymatic activity. Finally, the larger size of arginine than methionine could possibly modify the structure of the protein. These factors may have hindered the proper binding of the enzyme to its cofactor and thus contributed to the reduced enzymatic activity.

The fact that the double mutant (HMGRcGE680Q-M807R) exhibited the second lowest enzymatic activity of the mutants herein tested is not surprising. The two mutations were both found at sites where amino acids are highly conserved: the sequence of the cofactor binding site (DAMGMN) and that of the dimerization site (ENVIG).

The mutation made in the dimerization site caused glutamic acid to be replaced by glutamine in position 680. Although both amino acids are very similar in size, glutamic acid has a negative charge and glutamine a polar neutral charge. Glutamic acid has carboxylate (COO<sup>-</sup>) side chains that are potential proton acceptors, forming hydrogen bonds and thus the secondary structure of the protein ( $\beta$ -folded sheets or  $\alpha$ -helix).<sup>23</sup> It could possibly have a similar function as the Glu83 residue, which is highly conserved and participates in catalysis by transferring protons to Lys267. When glutamic acid carries out the decomposition of mevaldyl-CoA, its protonation and deprotonation confers different levels of energy to the reaction, and these are necessary for the enzymatic activity that gives rise to sterols.<sup>24</sup> Glu83 plays an important role in the formation of dimers and perhaps also in the active site of the enzyme due to its proximity to the S subdomain, which contains the cofactor binding site.<sup>3</sup> Glutamine is a glutamic acid amide afforded by the replacement of the hydroxyl of glutamic acid with an amine group.<sup>24</sup> Since it has a polar neutral charge, however, it might affect the interaction with the amino acids belonging to the ENVIG sequence. In the enzyme with both mutations, therefore, the proper formation of the dimers may not have taken place, leading to the inadequate binding of the enzyme to the cofactor and a consequent low enzymatic activity.

The proteins mutated in this work can be applied not only to improving *C. glabrata* as a model for research on drug resistance, but also to investigating the HMGR of additional species, such as *C. auris* and *C. haemulonii* that have recently emerged as pathogenic multi-drug resistant strains.<sup>25</sup> The

emergence of *Candida* infections associated with SARS-Cov2 gives greater emphasizes the urgency of developing antifungal agents for alternative targets.<sup>26</sup>

## Conclusions

The present study provides a model for examining the occurring mutations in the HMGR gene that cause drug resistance as a result of the selective pressure of antifungal agents on *Candida* spp. strains. Many *Candida* species exhibit multi-drug resistance and have recently emerged as causal agents of intrahospital outbreaks. The HMGR enzyme of *C. glabrata* (HMGR<sub>Cg</sub>), a multi-drug resistant opportunistic and pathogenic fungus, was herein expressed, mutated and modeled for the first time. Five point mutants were made at three highly conserved sites of the catalytic domain of HMGR: the dimerization, substrate binding and cofactor binding sites. Such mutations were expressed, detected and purified to verify their integrity. All the mutants exhibited significantly lower enzymatic activity and ligand affinity than wild-type HMGR<sub>Cg</sub>. The HMGR<sub>Cg</sub>E711Q mutant and the double mutant HMGR<sub>Cg</sub>E680Q-M807R displayed the lowest enzymatic activity and ligand affinity. The *in vitro* and *in silico* testing of these mutants gave insights into the function of specific amino acid residues in the catalytic site of the enzyme, especially glutamic acid. The current findings should certainly facilitate the creation of new mutants of HMGR to further explore catalysis, recognition, conformation, and dimerization mechanisms involved in the activity of the enzyme and the viability of *C. glabrata* and other opportunistic pathogenic fungi.

## Materials And Methods

### *Multiple sequence alignment of HMGR enzymes from different organisms*

The amino acid sequences were downloaded from the NCBI database (<https://www.ncbi.nlm.nih.gov/>) for the HMGR enzymes of the following organisms: *P. mevalonii* (WP\_016714288), *Arabidopsis thaliana* (NP\_177775), *Drosophila melanogaster* (NP\_732900), *Homo sapiens* (XP\_011541659), *Mus musculus* (NP\_001347095), *Rattus norvegicus* (NP\_037266), *Ustilago maydis* 521 (XP\_011389590), *S. pombe* (NP\_588235), *Yarrowia lipolytica* CLIB122 (XP\_503558), *Candida auris* (XP\_028890531), *Candida haemulonii* (XP\_025340375.1), *Clavispora lusitaniae* ATCC 42720 (XP\_002615608), *Meyerozyma guilliermondii* ATCC 6260 (XP\_001482757), *Debaryomyces hansenii* CBS767 (also called *Candida famata*) (XP\_458872), *Candida parapsilosis* (KAF6043359), *Candida orthopsilosis* Co 90–125 (XP\_003868277), *Candida tropicalis* MYA-3404 (XP\_002550050), *Candida albicans* SC5314 (XP\_713636), *Candida dubliniensis* CD36 (XP\_002417024), *Candida kefyr* (QGN16198), *Kluyveromyces lactis* NRRL Y-1140 (XP\_451740), *C. glabrata* CBS138 (XP\_449268), *Saccharomyces cerevisiae* S288c HMG1 (NP\_013636) and *S. cerevisiae* 2288c HMG2 (NP\_013555).<sup>27</sup> Once the sequences corresponding to the catalytic domain of such enzymes were downloaded, they were selected and subjected to multiple alignment in the Clustal Omega program.<sup>28</sup> The motif domains (structural motifs) were located with the ExpASy server, PROSITE (<https://prosite.expasy.org/>),<sup>29</sup> and visualized with the web server WebLogo (<http://weblogo.berkeley.edu/logo.cgi>).

### *Phylogenetic analysis of HMGR proteins from different organisms*

A phylogenetic tree was constructed with the sequences of the catalytic domain of the aforementioned twenty-four HMGRs in the MEGA6 program,<sup>30</sup> utilizing the maximum likelihood method and the WAG + G model. Additionally, a bootstrap replication of 100 was used to evaluate the reliability of the phylogenetic tree.

### *Homology modeling of *Candida glabrata* HMGR mutant proteins*

Fifteen models were generated for each of the five HMGRcG mutant proteins with the Modeller 9.24.<sup>31</sup> The models with the lowest discrete optimized protein energy (DOPE) score were selected and edited in Discovery Studio,<sup>32</sup> then subjected to a validation process to assess their stereochemical quality with the PROCHECK<sup>33</sup> tool integrated in the Structural Analysis and Verification Server (SAVES) (<https://servicesn.mbi.ucla.edu/SAVES/>). This tool also quantified the amino acid residues in the available regions of a Ramachandran plot.

### *Docking studies*

The ligands were downloaded from the PubChem server<sup>34</sup> in 2D format and transformed into 3D mol2 format in the Open Babel GUI program.<sup>35</sup> Kollman charges were assigned to the hydrogen atoms of the protein. Preparation of the docking parameters and molecular coupling of the five mutants to the ligands (HMG-CoA, simvastatin and alpha asarone) was carried out on AutoDock Tool 4.0.<sup>36</sup> The grid dimensions were set at 128 x 88 x 64 Å<sup>3</sup> with points separated by 0.375 Å, and the grid center was X=-10.517, Y = 14.058 and Z = 22.162. One hundred docking runs were made with the Lamarckian genetic algorithm and various parameters were estimated. The results were compared between ligands based on their lowest free coupling energy. Interactions were visualized with Discovery Studio.

### *Microorganisms and plasmids*

Transformation was achieved with the *Escherichia coli* DH10β strain and the overexpression of heterologous proteins with the *E. coli* BL21 strain. The plasmid pMAL-C2X-HMGRcG, which was previously obtained by our group and harbors the gene encoding the wild-type protein, was used as template DNA for the generation of the mutants.<sup>10</sup>

### *Culture media*

*E. coli* harboring the plasmids was grown in liquid Luria Bertani (LB) medium (1.0% casein peptone, 0.5% yeast extract and 0.5% NaCl) and solid LB medium with 1.5% bacteriological agar. These media were adjusted to pH 7.0 and supplemented with 100 µg/mL ampicillin. Culture media and antibiotics were acquired from Sigma Aldrich (St. Louis, MO, USA).

### *Mutagenic oligonucleotide design*

The mutagenic primers were designed manually, taking as templates the sequences of the dimerization site, the substrate binding site, and the cofactor binding site within the catalytic domain of the HMGR enzyme. Consideration was given to 18 base pairs to the left and 18 base pairs to the right of the codon

where the mutation was designed, resulting in a total of 39 nucleotides for each primer. Point mutations were made involving the following changes: glutamic acid to glutamine in the dimerization site (ENVIG) to provide E680Q, aspartic acid to glutamine in the substrate binding site (EGCLVAS) to afford E711Q, aspartic acid to alanine in the cofactor binding site (DAMGMN) to furnish (D805A), and methionine to arginine in the cofactor binding site to yield M807R. The double mutation of E680Q-M807R was formed by the respective single point mutations.

The oligonucleotides herein designed were synthesized at the Institute of Biotechnology of the National Autonomous University of Mexico (UNAM). The melting temperature ( $T_m$ ) of the oligonucleotides was calculated after their synthesis, using the bioinformatics program Oligo Analyzer from Integrated DNA Technologies (IDT) (<https://www.idtdna.com/pages/tools/oligoanalyzer>).

Table 3 shows the original sequence (wild-type HMGRc<sub>g</sub>) and the mutagenic oligonucleotides. The codon of the amino acid to be mutated is illustrated in red, and the change made is underlined.

Table 3

Oligonucleotides designed to obtain the following point mutants: E680Q, E711Q, D805A, M807R and E680Q-M807R.

Mutated aa	Direction	39 pb Oligonucleotides sequences	Tm	%GC
E680	Fw	5' GTCTTTGGTGCTTGTGTTGT <b>G</b> AAATGTGATTGGTTACATG 3'	75.4	62.9
E680Q	Fw	5' GTCTTTGGTGCTTGTGTTGT <b>C</b> AAATGTGATTGGTTACATG 3'	75.4	62.9
E680Q	Rv	5' CATGTAACCAATCACATTT <b>T</b> GACAACAAGCACCAAAGAC3'	75.4	62.9
E711	Fw	5' ATCCCTATGGCCACAAC <b>T</b> GAAGGTTGCTTGGTTGCATCT3'	80.1	67.1
E711Q	Fw	5' ATCCCTATGGCCACAAC <b>C</b> AAGGTTGCTTGGTTGCATCT 3'	80.1	67.1
E711Q	Rv	5'AGATGCAACCAAGCAAC <b>C</b> TTGAGTTGTGGCCATAGGGAT 3'	80.1	67.1
D805	Fw	5' TTTAGAACTACAAC <b>T</b> GGT <b>G</b> ATGCGATGGGTATGAATATG 3'	73.0	62.9
D805A	Fw	5' TTTAGAACTACAAC <b>T</b> GGT <b>G</b> CTGCGATGGGTATGAATATG 3'	74.2	63.9
D805A	Rv	5' CATATTCATACCCATCGC <b>A</b> GCACCAGTTGTAGTTCTAAA 3	74.2	63.9
M807	Fw	5'ACTACAAC <b>T</b> GGTGATGCG <b>A</b> TGGGTATGAATATGATTTCT3	73.5	62.9
M807R	Fw	5'ACTACAAC <b>T</b> GGTGATGCG <b>A</b> GGGTATGAATATGATTTCT3	74.1	63.9
M807R	Rv	5'AGAAATCATATTCATAC <b>C</b> CTCGCATCACCAGTTGTAGT3'	74.1	63.9

#### Generation of HMGRGc point mutants by PCR

The E680Q, E711Q and D805A point mutants were generated by PCR with a "Quick Change" commercial kit (Thermo Fisher Scientific™, USA), following the manufacturer's instructions with some modifications. This procedure is based on a PCR reaction with two complementary and antiparallel oligonucleotides and the appropriate DNA polymerase to achieve the desired mutation. Each oligonucleotide hybridizes with one of the two strands of the plasmid to be amplified. The plasmid was obtained that leads to the sequence to be mutated (pMAL-c2X-HMGRGc), which was used as the template DNA. Mutants M807R and E680Q-M807R were produced by inverse PCR, using the plasmid pMBP-HMGRGc as the template DNA.<sup>10,11</sup> For the double mutant, the plasmid DNA of the rec-HMGRGc-E680Q mutant and the mutagenic oligonucleotide M807R served as the template DNA.

Once the reaction conditions were established and developed, the amplicon was digested with the Dpn-I enzyme (Thermo Fisher Scientific™-USA). *E. coli* DH10β cells were then transformed with the digested PCR product. Subsequently, *E. coli* cells were plated on LB agar with ampicillin (100 µg/ml) and incubated at 37°C for 24 h. The transforming colonies were selected for the extraction of plasmid DNA. Plasmids were purified with the ZymoPURE™ plasmid Miniprep Kit (Zymo Research, CA, USA) and confirmed by sequencing them according to the Sanger method, finding the presence of the desired mutations (Macrogen®, Seoul Korea).

#### *Expression, purification and detection of wild-type and mutant recombinant proteins*

Once the presence of the desired mutations was confirmed by sequencing the corresponding plasmids, the recombinant proteins were expressed. Briefly, *E. coli* BL21 cells were transformed with the mutated DNA by growing the cells containing the fusion plasmid in LB medium plus ampicillin (100 µg/mL) and 0.2% glucose until reaching an optical density of 0.6 at 600 nm. IPTG was added immediately (0.3 mM final concentration) to induce the expression of the protein, a process carried out at 37°C for 4 h. Upon completion of this time, cells were harvested at 4000 x g for 20 min at 4°C. The cells were mechanically broken by using glass beads and a vortex, and then the cell pack was dissolved in a column buffer (1 M Tris-HCl, pH 7.4, 11.7 g NaCl, 0.5 M EDTA and 154 mg DTT) to obtain a cell-free extract. The cells were disrupted for 20 min, alternating every other 30 sec on and off ice. The cell lysate was centrifuged at 18000 g for 20 min and the supernatant (cell-free extract) was recovered. The protein was purified by affinity column chromatography with amylose resin (New England Biolabs, USA). The wild-type and mutant proteins were eluted with a buffer supplemented with 10 mM maltose. Fractions were collected to determine the HMGRcG activity and protein concentration by the Lowry method. The expression and the successful purification of the mutant proteins was visualized by means of 10% SDS-PAGE stained with Coomassie blue. The mutated proteins were detected by Western blot with the anti-MBP monoclonal antibody (New England Biolabs, USA), according to the manufacturer's specifications.

#### *HMGR enzymatic activity assay*

The enzymatic activity of the five mutants was quantified by the method of Bischoff and Rodwell,<sup>37</sup> beginning with the elaboration of a reaction mixture containing 10 mM HMG-CoA, 50 mM Tris-HCl regulator, injectable water, 9 µg of the protein of the respective mutant, and 10 mM NADPH. The cofactor (NADPH) was oxidized by the catalytic subunit of HMGR in the presence of the substrate HMG-CoA, causing a decrease in absorbance, which was monitored at 340 nm for 10 min. Reagents were purchased from Sigma Aldrich (St Louis, MO, USA). One unit of specific activity was defined as the amount of enzyme that oxidizes 1 µmol of NADPH to NADP + per minute per milligram of protein. All spectrophotometric readings were made on a BioSpectrometer® kinetic apparatus (Eppendorf AG, Germany).

## **Declarations**

## **Acknowledgments**

The authors would like to thank Bruce Allan Larsen for proofreading the manuscript.

## Author Contributions

DAP wrote and performed experimental assays, VFM and WGI performed experimental assays, CHR and JAIG reviewed the manuscript and LVT coordinated, supervised and reviewed the manuscript.

## Funding

This work was supported by CONACYT [grant number CB-283225], SIP-IPN [grant numbers 20210508, 20200775, and 20200204]. DMAP was the recipient of fellowships from CONACyT and BEIFI-IPN. VFM and WGB are recipients of fellowships from BEIFI-IPN. JAI, CHR and LVT received support from COFAA-IPN, EDI-IPN and SNI CONACyT. JAI and LVT were hired through the “Programa Institucional de Contratación de Personal Académico de Excelencia IPN”.

## Competing interests

None.

## References

1. Friesen, J. A. & Rodwell, V. W. The 3-hydroxy-3-methylglutaryl coenzyme-A (HMG-CoA) reductases. *Genome. Biol*, **5**, 248 (2004).
2. Nawarskas, J. J. HMG-CoA reductase inhibitors and coenzyme Q10. *Cardiol. Rev*, **13**, 76–79 (2005).
3. Istvan, E. S. & Deisenhofer, J. Structural mechanism for statin inhibition of HMG-CoA reductase. *Science*, **292**, 1160–1164 (2001).
4. Licata, A. *et al.* Liver and Statins: A Critical Appraisal of the Evidence. *Curr. Med. Chem*, **25**, 5835–5846 (2018).
5. Argüelles, N. *et al.* Design, synthesis, and docking of highly hypolipidemic agents: *Schizosaccharomyces pombe* as a new model for evaluating alpha-asarone-based HMG-CoA reductase inhibitors. *Bioorg. Med. Chem*, **18**, 4238–4248 (2010).
6. Mendieta, A. *et al.* Synthesis and highly potent hypolipidemic activity of alpha-asarone- and fibrate-based 2-acyl and 2-alkyl phenols as HMG-CoA reductase inhibitors. *Bioorg. Med. Chem*, **22**, 5871–5882 (2014).
7. Andrade-Pavón, D. *et al.* The 3-hydroxy-3-methylglutaryl coenzyme-A reductases from fungi: a proposal as a therapeutic target and as a study model. *Rev. Iberoam. Micol*, **31**, 81–85 (2014).
8. Pristov, K. E. & Ghannoum, M. A. Resistance of *Candida* to azoles and echinocandins worldwide. *Clin. Microbiol. Infect*, **25**, 792–798 (2019).
9. Subhan, M., Faryal, R. & Macreadie, I. Statin resistance in *Candida glabrata*. *Biotechnol. Lett*, **40**, 1389–1394 (2018).

10. Andrade-Pavón, D. *et al.* Recombinant 3-Hydroxy 3-Methyl Glutaryl-CoA Reductase from *Candida glabrata* (Rec-CgHMGR) Obtained by Heterologous Expression, as a Novel Therapeutic Target Model for Testing Synthetic Drugs. *Appl. Biochem. Biotechnol*, **182**, 1478–1490 (2017).
11. Andrade-Pavón, D. *et al.* Inhibition of recombinant enzyme 3-hydroxy-3-methylglutaryl-CoA reductase from *Candida glabrata* by  $\alpha$ -asarone-based synthetic compounds as antifungal agents. *J. Biotechnol*, **292**, 64–67 (2019).
12. Wang, Y., Darnay, B. G. & Rodwell, V. W. Identification of the principal catalytically important acidic residue of 3-hydroxy-3-methylglutaryl coenzyme A reductase. *J. Biol. Chem*, **265**, 21634–21641 (1990).
13. Darnay, B. G., Wang, Y. & Rodwell, V. W. Identification of the catalytically important histidine of 3-hydroxy-3-methylglutaryl-coenzyme A reductase. *J. Biol. Chem*, **267**, 15064–15070 (1992).
14. Jordan-Starck, T. C. & Rodwell, V. W. Role of cysteine residues in *Pseudomonas mevalonii* 3-hydroxy-3-methylglutaryl-CoA reductase. Site-directed mutagenesis and characterization of the mutant enzymes. *J. Biol. Chem*, **264**, 17919–21793 (1989).
15. Darnay, B. G. & Rodwell, V. W. His865 is the catalytically important histidyl residue of Syrian hamster 3-hydroxy-3-methylglutaryl-coenzyme A reductase. *J. Biol. Chem*, **268**, 8429–8435 (1993).
16. Frimpong, K. & Rodwell, V. W. Catalysis by Syrian hamster 3-hydroxy-3-methylglutaryl-coenzyme A reductase. Proposed roles of histidine 865, glutamate 558, and aspartate 766. *J. Biol. Chem*, **269**, 11478–11483 (1994).
17. Gabaldón, T. *et al.* Comparative genomics of emerging pathogens in the *Candida glabrata* clade. *BMC. Genomics*, **14**, 623 (2013).
18. Ahmad, K. Genome structure and dynamics of the yeast pathogen. *Candida glabrata*. *Yeast*, **14**, 529–535 (2014).
19. Istvan, E. S., Palnitkar, M., Buchanan, S. K. & Deisenhofer, J. Crystal structure of the catalytic portion of human HMG-CoA reductase: insights into regulation of activity and catalysis. *The EMBO. Journal*, **19**, 819–830 (2000).
20. Endo, A., Kuroda, M. & Tanzawa, K. Competitive inhibition of 3-hydroxy-3-methylglutaryl-coenzyme A reductase by ML-236A and ML-236B fungal metabolites, having hypolesterolemic activity. *FEBS. Lett*, **72**, 323–326 (1976).
21. Wu, G. Amino acids: metabolism, functions, and nutrition. *Amino Acids*, **37**, 1–17 (2009).
22. Li, X. *et al.* The role of methionine on metabolism, oxidative stress, and diseases. *Amino Acids*, **49**, 2091–1098 (2017).
23. Taylor, M., Nelson, J., Suero, M. & Gaunt, M. A protein functionalization platform based on selective reactions at methionine residues. *Nature*, **562**, 563–568 (2018).
24. Taberner, L., Bochar, D., Rodwell, V. & Stauffacher, C. Substrate-induced closure of the flap domain in the ternary complex structures provides insights into the mechanism of catalysis by 3-hydroxy-3-methylglutaryl-CoA reductase. *Proc. Natl. Acad. Sci.* **96**, 7167–7171(1999).

25. Reséndiz- Sánchez, J., Ortiz-Alvarez, J., Casimiro-Ramos, A. & Hernández-Rodríguez, C. & Villa-Tanaca, L. First report of a catheter-related bloodstream infection by *Candida haemulonii* in a children's hospital in Mexico City. *Int. J. Infect. Dis*, **92**, 123–126 (2020).
26. Lai, C. C., Chen, S. Y., Ko, W. C. & Hsueh, P. R. Increased antimicrobial resistance during COVID-19 pandemic. *International. Journal. of. Antimicrobial. Agents*, **57**, 106324 (2021).
27. Sharma, S. *et al.* The NCBI BioCollections Database. **Database.1–1**(2019).
28. Sievers, F. *et al.* Fast, scalable generation of high-quality protein multiple sequence alignments using Clustal Omega. *Mol. Syst. Biol*, **7**, 539 (2011).
29. Gasteiger, E. *et al.* ExPASy: The proteomics server for in-depth protein knowledge and analysis. *Nucleic Acids Res*, **31**, 3784–3788 (2003).
30. Tamura, K., Stecher, G., Peterson, D., Filipski & Kumar, A. S. MEGA6: Molecular Evolutionary Genetics Analysis version 6.0. *Mol. Biol. Evol*, **30**, 2725–2729 (2013).
31. Webb, B. & Sali, A. Comparative Protein Structure Modeling Using MODELLER. *Curr. Protoc. Bioinformatics*. 54, 5.6.1–5.6.37(2016).
32. Dassault Systems, B. I. O. V. I. A. *Discovery Studio Modeling Environment, Release 2017* (Dassault Systems, San Diego, 2016).
33. Laskowski, R. A., MacArthur, M. W., Moss, D. S. & Thornton, J. M. PROCHECK - a program to check the stereochemical quality of protein structures. *J. App. Cryst*, **26**, 283–291 (1993).
34. Wang, Y. *et al.* PubChem BioAssay: 2017 update. *Nucleic. Acids. Res*, **45**, D955–D963 (2017).
35. O'Boyle, N. M. *et al.* Open Babel: An open chemical toolbox. *J. Cheminform*, **3**, 33 (2011).
36. Morris, G. M. *et al.* AutoDock4 and AutoDockTools4: Automated docking with selective receptor flexibility. *J. Comput. Chem*, **30**, 2785–2791 (2009).
37. Bischoff, K. M. & Rodwell, V. W. Biosynthesis and characterization of (S)- and (R)-3-hydroxy-3-methylglutaryl coenzyme A. *Biochem. Med. Metab. Biol*, **48**, 149–158 (1992).

## Figures

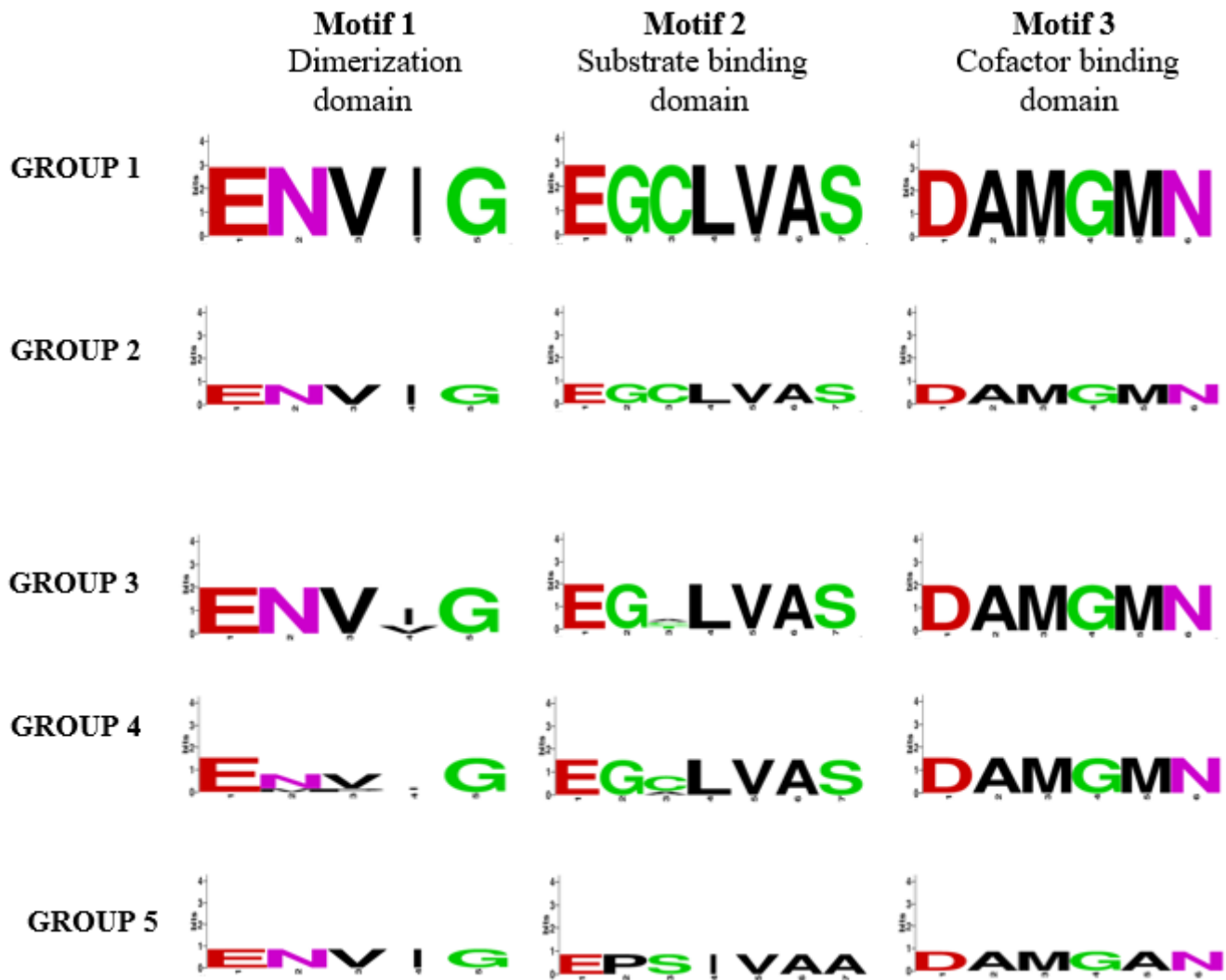
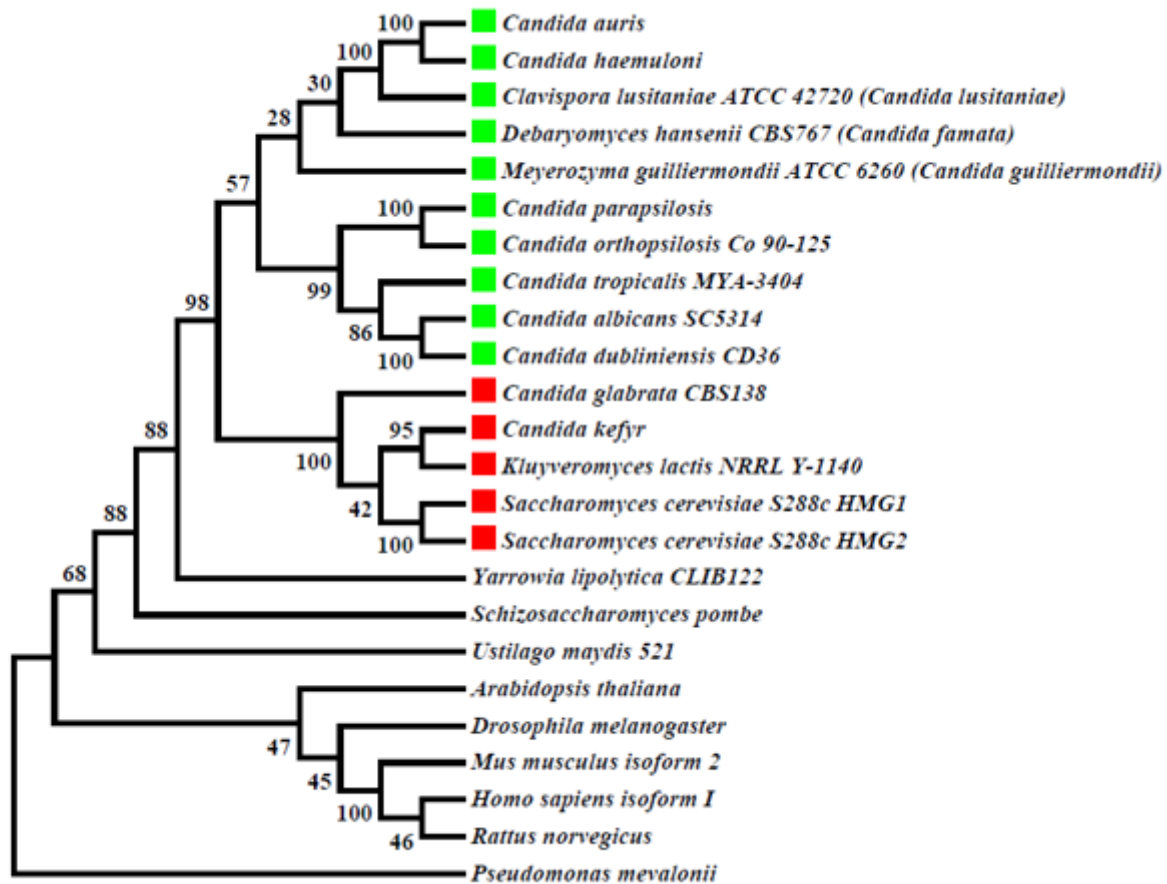


Figure 1

Sequence logos of the conserved motifs found in the catalytic domain of the HMGRs of different organisms. Multiple alignments were performed with Clustal Omega and the consensus logos were generated with WebLogo. Group 1 (*Candida auris*, *Candida haemulonii*, *Clavispora lusitaniae* ATCCC 42720, *Debaryomyces hansenii* CBS767, *Meyerozyma guilliermondii* ATCC 6260, *C. parapsilosis*, *C. orthopsilosis* Co 90-125, *C. tropicalis* MYA-3404, *C. albicans* SC5314, and *C. dubliniensis* CD36); group 2 (*C. glabrata* CBS138, *C. kefyr*, *Kluyveromyces lactis* NRRL Y-1140, *Saccharomyces cerevisiae* S288c HMG1, and *S. cerevisiae* S288c HMG2); group 3 (*Yarrowia lipolytica* CLIB122, *Schizosaccharomyces pombe*, and *Ustilago maydis*); group 4 (*Drosophila melanogaster*, *Mus musculus*, *Homo sapiens*, and *Rattus norvegicus*); and group 5 (*Pseudomonas mevalonii*).



**Figure 2**

Phylogenetic analysis of the catalytic domain of the HMGR enzymes of different organisms, conducted in the MEGA6 program with the maximum likelihood method and the WAG+G model. The percentage of replicated trees in which the associated taxa are grouped in the 100 bootstrap replicates is shown next to the branches. The phylogenetic tree is drawn to scale, with the length of the branches representing the corresponding evolutionary distances. The species in the clade that encompasses *Candida glabrata* (in red) developed based on whole genome duplication (WGD). In the clade containing *Candida albicans* (in green), the species developed based on genetic code transition (GCT).

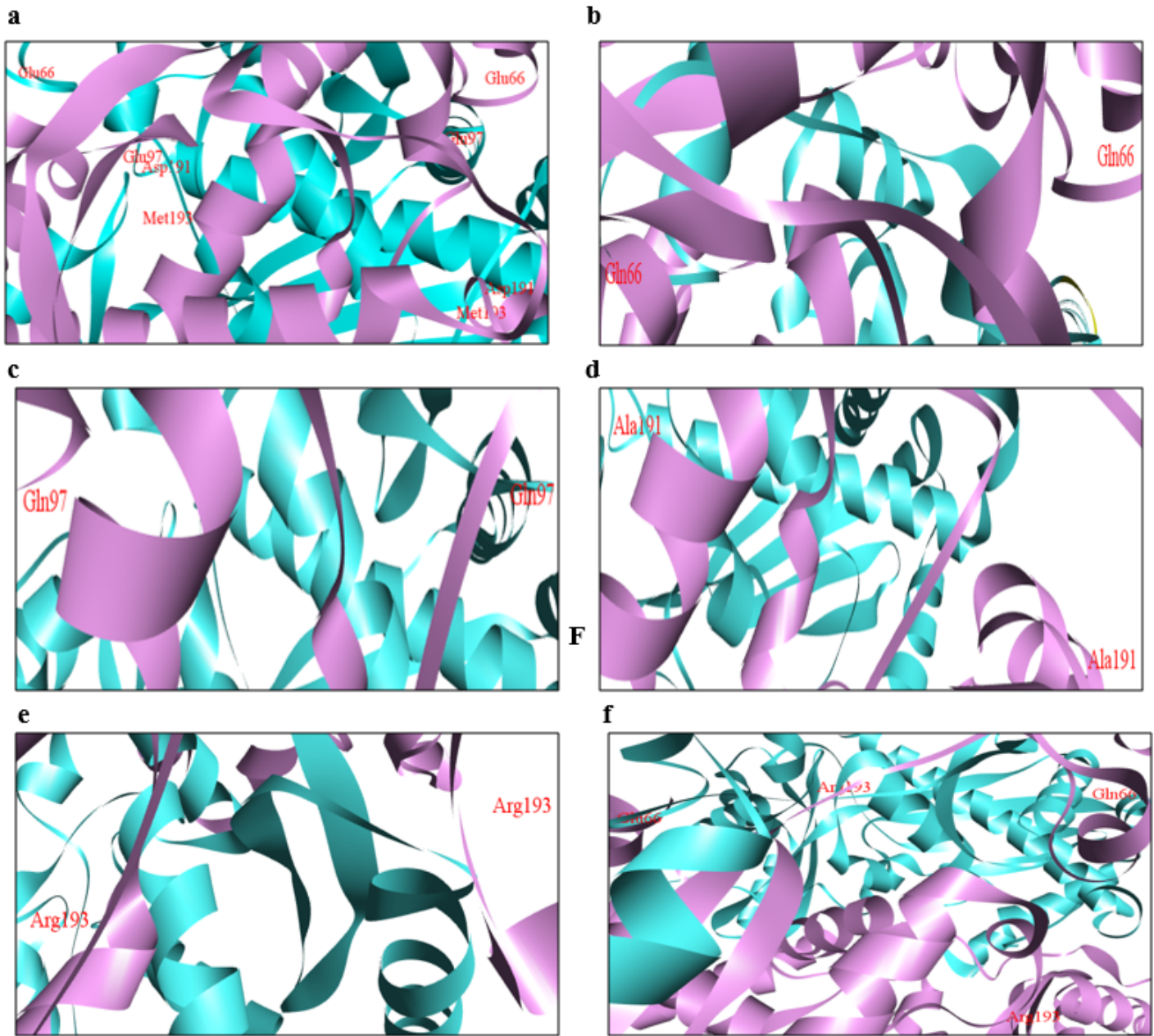


**Figure 3**

Structural modeling of the conformational differences between wild-type and mutant HMGR proteins of *Candida glabrata* (HMGRcG), in flat ribbon representation. (a) Wild-type HMGRcG, (b) mutant HMGRcG680Q, (c) mutant HMGRcG711Q, (d) mutant HMGRcGD805A, (e) mutant HMGRcGM807R, and (f) mutant HMGRcG680Q-M807R. The  $\alpha$  monomer is depicted in pink, the  $\beta$  monomer in cyan, and the mutation in red.

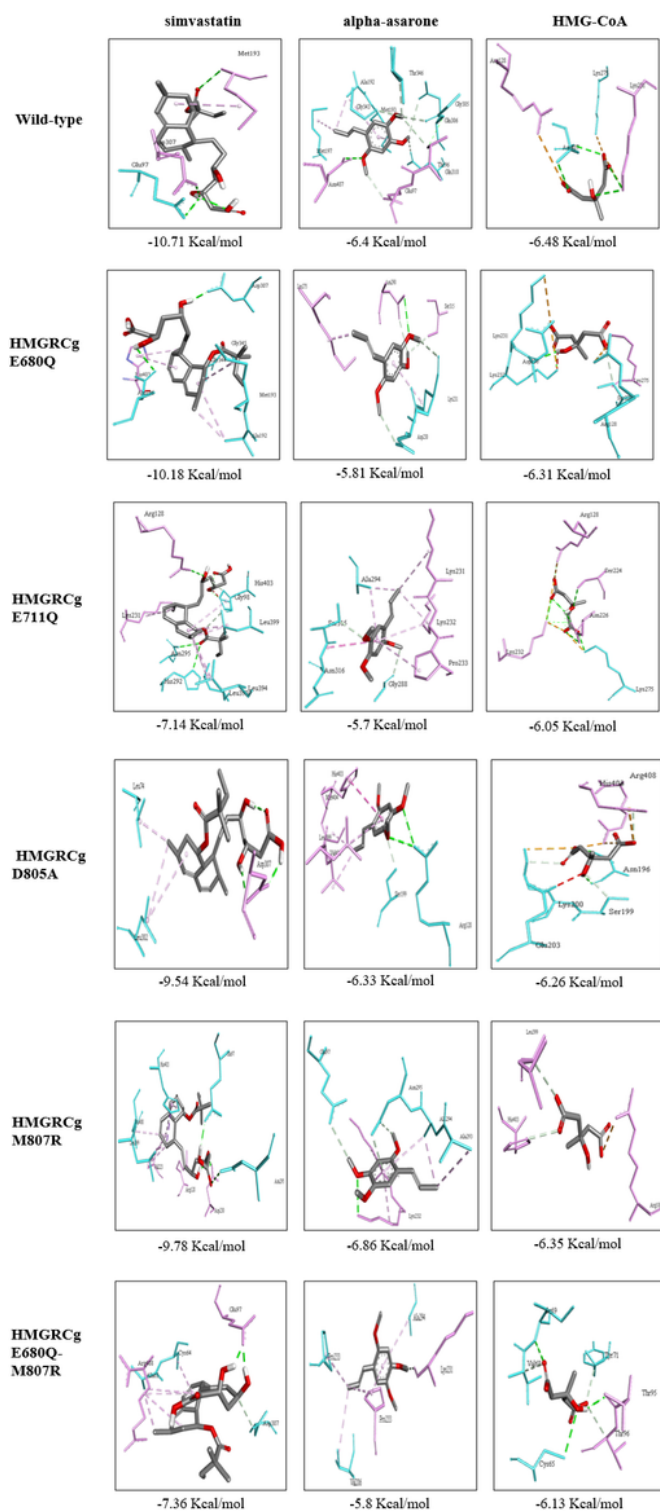


**Figure 4**

3D representation of the molecular interactions of simvastatin, alpha-asarone and HMG-CoA with the active site of the wild-type and mutant HMGRcG proteins. The amino acids of monomer  $\alpha$  are depicted in pink and those of monomer  $\beta$  in cyan. The dotted lines denote the following bonds: conventional hydrogen (green), carbon-hydrogen (gray), pi-anion (orange) and pi-alkyl (pink). Interaction energies are expressed in Kcal/mol.

HMGRcG WT                    ACTACGATTATGATAGAGTCTTTGGTGCTTGTGTGAAATGTGATTGGTTACATGCCAT  
 HMGRcGE680Q                ACTACGATTATGATAGAGTCTTTGGTGCTTGTGTGCAATGTGATTGGTTACATGCCAT

HMGRcG WT                    CCACAAC TGAGGTTGCTTGGTTGCATCTGCCATGCGTGGTTGCAAGGCTATAAATGCCG  
 HMGRcGE711Q                CCACAAC CAGGTTGCTTGGTTGCATCTGCCATGCGTGGTTGCAAGGCTATAAATGCCG

HMGRcG WT                    CTGCTCTTGCTGGTGACTTACTATTTATTCGTTTTAGAACTACAAC TGGT GATGCGATGG  
 HMGRcGD805A                CTGCTCTTGCTGGTGACTTACTATTTATTCGTTTTAGAACTACAAC TGGT GCTGCGATGG

HMGRcG WT                    TTTGTTTTAACACAAATTCAACACCTTTAGAAATCATATTCATACC CATCGCATCACCAG  
 HMGRcGM807R                TTTGTTTTAACACAAATTCAACACCTTTAGAAATCATATTCATACC CCTCGCATCACCAG  
 HMGRcGE680Q-M807R        TTTGTTTTAACACAAATTCAACACCTTTAGAAATCATATTCATACC CCTCGCATCACCAG

HMGRcG WT                    TCACATT TTCACAACAAGCACCAAGAATCTATCAAATCGTATTCTTGTAAGGAAAACA  
 HMGRcGM807R                -----  
 HMGRcGE680Q-M807R        TCACATT TTGACAACAAGCACCAAGAATCTATCAAATCGTAATTTTGTTAGGGA---

**Figure 5**

Alignment of the nucleotide sequences, comparing wild-type *Candida glabrata* HMGR (HMGRcG) to the mutants HMGRcGE680Q, HMGRcGE711Q, HMGRcGD805A, HMGRcGM807R, and HMGRcGE680Q-M807R. The triplets coding for the amino acids that were the target of mutation are highlighted in yellow. The mutated nucleotide base (marked in fuchsia) changed from G-C for HMGRcGE680Q and HMGRcGE711Q, from A-C for HMGRcGD805A and HMGRcGM807R, and from A-C and C-G for HMGRcGE680Q-M807R. The alignment was performed in the MUSCLE program.

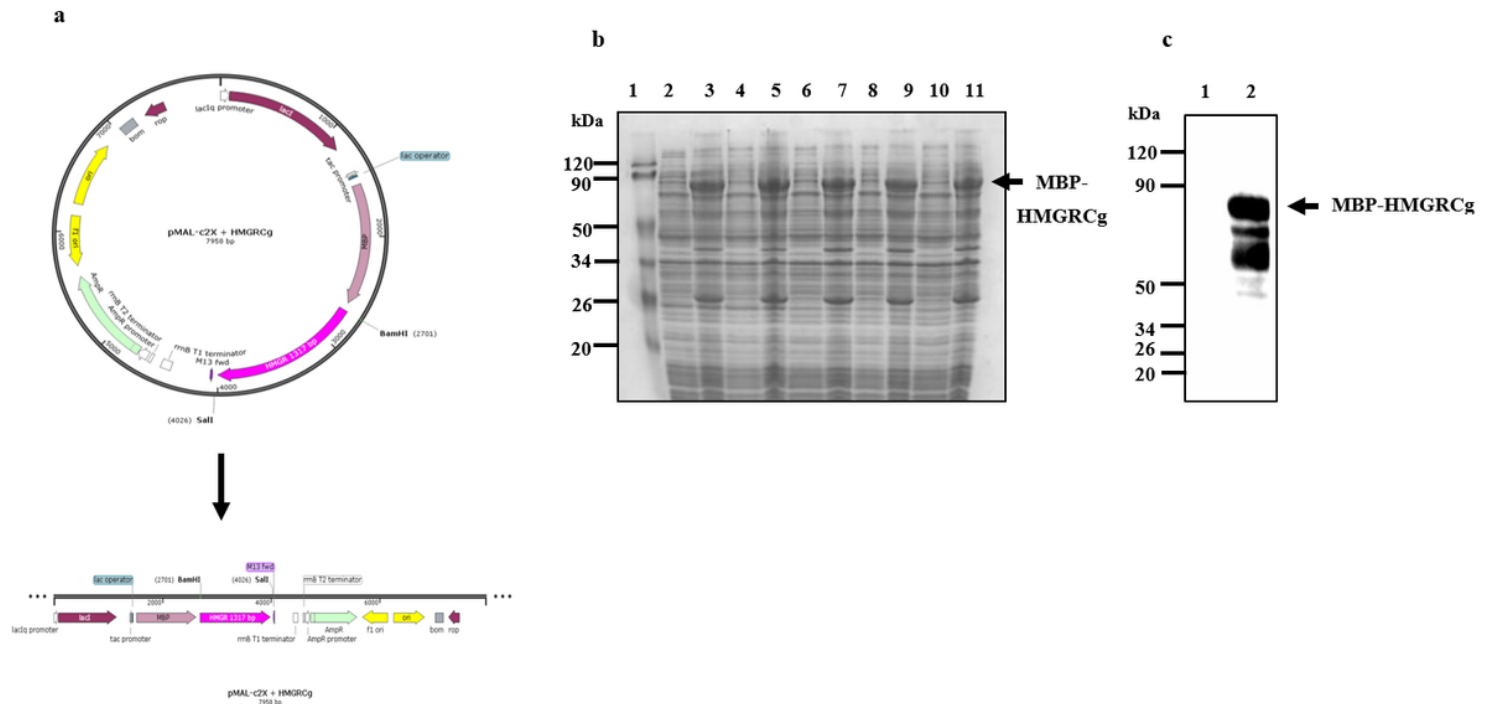


**Figure 6**

Graphic representation, overexpression, and detection of the recombinant HMGRcG E680Q, HMGRcG E711Q, HMGRcG 805A, HMGRcG M807R and HMGRcG E680Q-M807R mutants. (a) Cartoon illustration of the p-MBP-HMGRcG (where MBP refers to the maltose-binding protein) used to obtain and express mutant HMGRcG proteins. (b) SDS-PAGE of the expression of the mutated proteins: Lane 1, molecular weight marker; lanes 2, 4, 6, 8 and 10, extract of cells before induction; lanes 3, 5, 7, 9 and 11, extract of cells after induction with IPTG. Full-length gel is included in a Supplementary Information (Fig. S4a). (c) Example of the verification of protein identity by Western blot based on anti-MBP antibodies: Lane 1, molecular weight marker; lane 2, uninduced cell extract; lane 3, induced cell extract. Full-length blot is included in a Supplementary Information (Fig. S4b).

## Supplementary Files

This is a list of supplementary files associated with this preprint. Click to download.

- [SupplementaryInfoFile240621.pdf](#)